Earth Planets Space, **64**, 1199–1207, 2012

Analysis of seismic magnitude differentials (m_b–M_w) across megathrust faults in the vicinity of recent great earthquakes

Teresa M. Rushing and Thorne Lay

University of California Santa Cruz, Santa Cruz, California 95064, U.S.A.

(Received December 27, 2011; Revised August 20, 2012; Accepted August 21, 2012; Online published January 28, 2013)

Spatial variations in underthrusting earthquake seismic magnitude differentials ($m_b - M_w$) are examined for plate boundary megathrusts in the vicinity of the 26 December 2004 Sumatra-Andaman (M_w 9.2), 2010 Maule, Chile (M_w 8.8), and 11 March 2011 Tohoku, Japan (M_w 9.1) great earthquakes. The magnitude differentials, corrected for ω-squared source spectrum dependence on seismic moment, provide a first-order probe of spatial variations of frequency-dependent seismic radiation. This is motivated by observations that the three great earthquakes all have coherent short-period radiation from the down-dip portions of their ruptures as imaged through back-projections, but little coherent short-period energy from shallower regions where large coseismic slip occurred. While there is substantial scatter in the magnitude measures, all three regions display some increase in relative strength of short-period seismic waves with depth, with the pattern being strongest for Sumatra and Japan where the deeper portion of the seismogenic zone is below the overriding crust. Other regions such as the Kuril Islands, Aleutians, Peru, and Southern Sumatra/Sumba show little, if any, depth pattern in the magnitude differentials. Variation in material and frictional properties over particularly wide seismogenic megathrusts likely produce the depth-dependence observed in both $m_b - M_w$ residuals and great earthquake seismic radiation.

Key words: 2011 Tohoku earthquake, megathrust faults, subduction zones, great earthquake rupture process, tsunami earthquakes.

1. Introduction

Seismic radiation from earthquakes on interplate megathrust faults has long been known to vary spatially (e.g., Lay *et al*., 1982; Kanamori, 1986). The most dramatic example of this is provided by "tsunami earthquakes", which are large tsunamigenic thrust faulting earthquakes that rupture shallow (<15 km) depths of megathrusts and have anomalously low surface wave and body wave magnitudes relative to their long-period moment magnitudes (M_w) (Kanamori, 1972). The deficiency in short-period seismic energy release is generally attributed to unusually low rupture expansion rate or slow particle dislocation velocities that may result from the presence of low rigidity sediments and pore fluids in the fault zone at shallow depths (e.g., Kanamori and Kikuchi, 1993; Newman and Okal, 1998; Polet and Kanamori, 2000; Lay and Bilek, 2007). Large tsunami earthquakes are relatively rare, but widespread smaller underthrusting ruptures at depths less than 15 km can exhibit similarly anomalous long source durations relative to typical sources (Bilek and Lay, 1999, 2002; Lay and Bilek, 2007; Bilek, 2007; Bilek *et al*., 2012).

Large earthquake ruptures deeper on the megathrust also vary in complexity of seismic radiation, which is generally attributed to heterogeneity in fault strength and/or frictional properties (e.g., Lay *et al*., 1982; Kanamori, 1986; Kikuchi and Fukao, 1987; Yamanaka and Kikuchi, 2004; Lay *et al*., 2012). Spatial variations of megathrust rupture process are observed both along trench strike and along slab dip (e.g., Yomogida *et al*., 2011). The underlying causes of the variability are uncertain, but likely contributing factors include variations of temperature, normal stress, fault zone fluids, megathrust geometry and roughness, sediments, and fault zone rock properties.

Several recent great megathrust earthquakes have ruptured across entire seismogenic widths, and availability of extensive seismic data has enabled the first detection of frequency-dependent radiation as a function of depth on the fault during the ruptures (e.g., Lay *et al*., 2012). This has been demonstrated for the 26 December 2004 Sumatra-Andaman (M_w 9.2), 27 February 2010 Maule, Chile (M_w 8.8), and 11 March 2011 Tohoku, Japan (M_w 9.1) earthquakes (Fig. 1), as discussed below.

The cause of this depth-variation in seismic radiation is not yet fully understood, and it is important to establish whether it is produced by distinctive rupture processes that only occur during great earthquakes or is a manifestation of material properties and stress heterogeneity that also affects smaller events. We address this question by considering whether seismic magnitude measures that characterize relative short-period and long-period seismic radiation for smaller events on megathrusts also indicate depth-dependent patterns. Seismic magnitudes provide limited characterization of the source spectra, but evidence is found for depth variation in magnitude differentials consistent with the seismic radiation observations for great earthquake

doi:10.5047/eps.2012.08.006

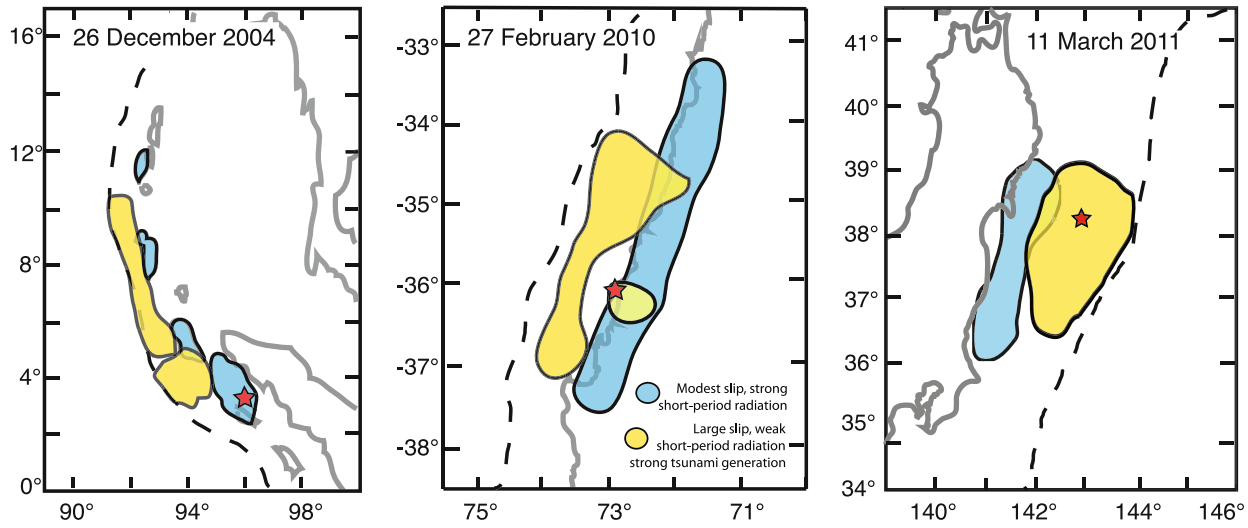

Fig. 1. Schematic patterns of coherent short-period radiation and large coseismic slip regions for the great 26 December 2004 Sumatra (M_w 9.2), 27 February 2010 Chile (M_w 8.8) and 11 March 2011 Tohoku, Japan (M_w 9.0) earthquakes. Regions of largest fault displacements (yellow) and regions of coherent short-period (∼1 s) teleseismic radiation (blue) are indicated. The dashed lines are the position of the subduction zone trench, the thick gray lines are coastlines, and the red stars are the epicenters. In each case the coherent short-period radiation comes from down-dip, closer to the coast (30–50 km deep), while the large slip zones are in the upper 30 km, extending seaward toward the trench. Short-period energy is located by network back-projections, while main slip regions are located by inverting seismic, geodetic, and/or tsunami observations, as described in the text for each event. (From Lay *et al*., 2012).

ruptures near the 2004 Sumatra-Andaman, 2010 Maule, Chile and 2011 Tohoku, Japan events.

2. Depth Variations of Seismic Radiation for Great Earthquakes

Characterizing frequency-dependent variations of seismic radiation on megathrusts is challenging due to the intrinsic variability and size scaling of earthquakes, the limitations on coverage and bandwidth of seismic observations, and the spatial averaging effects of seismic waves. The recent evidence for distinctive seismic radiation from the deeper portion of the seismogenic zone for the three great earthquakes in Fig. 1 has come from back-projection of large aperture network recordings of teleseismic *P* waves, following methods introduced by Ishii *et al*. (2005). Coherent localized sources of short-period (∼1 s) radiation (Fig. 1) have been imaged for the 2004 Sumatra-Andaman earthquake (e.g., Ishii *et al*., 2005; Krüger and Ohrnberger, 2005; Lay *et al*., 2012), 2010 Chile earthquake (Lay *et al*., 2010; Kiser and Ishii, 2011; Wang and Mori, 2011b; Koper *et al*., 2012), and 2011 Tohoku earthquake (Ishii, 2011; Koper *et al*., 2011a, b; Meng *et al*., 2011; Wang and Mori, 2011a; Yao *et al*., 2011; Zhang *et al*., 2011). For the 2011 Tohoku earthquake the sources of teleseismic short-period radiation are located close to sources of strong ground motion accelerations determined by Kurahashi and Irikura (2011), suggesting a common origin.

The source locations for coherent ∼1 s short-period radiation to teleseismic distances are found to be in the down-dip portions (30–55 km deep) of the megathrusts. This is deeper than the regions of large coseismic slip determined by many inversions and modeling of seismic, geodetic, and tsunami observations for the 2004 Sumatra-Andaman earthquake (e.g., Ammon *et al*., 2005; Vigny *et al*., 2005; Chlieh *et al*., 2007; Rhie *et al*., 2007), 2010 Chile earthquake (e.g., Lay *et al*., 2010; Lorito *et al*., 2011; Pollitz *et al*., 2011b; Vigny *et al*., 2011), and 2011 Tohoku earthquake (e.g., Ammon *et al*., 2011; Fujii *et al*., 2011; Hayes, 2011; Ide *et al*., 2011; Iinuma *et al*., 2011; Ito *et al*., 2011; Koketsu *et al*., 2011; Lay *et al*., 2011; Lee *et al*., 2011; Maeda *et al*., 2011; Ozawa *et al*., 2011, 2012; Pollitz *et al*., 2011a; Shao *et al*., 2011; Simons *et al*., 2011; Yokota *et al*., 2011; Yoshida *et al*., 2011; Yue and Lay, 2011; Wei *et al*., 2012).

The various finite-fault rupture models differ in precise placement of slip on the fault, notably with geodetic inversions locating the slip closer to the coast than do seismic inversions for the 2010 Chile and 2011 Tohoku events. However, the overall offset of regions with large slip from locations of sources of short-period coherent radiation is quite systematic, as summarized in Fig. 1. The shallowest portion of the 2011 Tohoku rupture appears to have behaved as in a tsunami earthquake, and very large slip of 40–80 m has been estimated offshore near the trench, but no coherent 1-s sources of short-period radiation are imaged there. It is not yet resolved whether the 2010 Chile event ruptured to the trench, but recent geodetic inversions (e.g., Vigny *et al*., 2011) favor large slip being relatively far offshore as in some seismic models (Lay *et al*., 2010), although not peaking near the trench as for the 2011 Tohoku rupture. Recent tsunami modeling indicates that the same is true for the 2004 Sumatra-Andaman event (Poisson *et al*., 2011).

3. m_b–M_w Differential Magnitude Patterns

Spatially isolating regions of distinct source spectrum within a great rupture is very difficult, and back-projection methods do not provide robust absolute amplitude constraints on the source spectrum at any depth. Systematic analysis of rupture processes or spectra of moderate and small events on the megathrust is a worthwhile, but massive undertaking (e.g., Bilek and Lay, 1999; Bilek *et al*., 2012),

so we take an alternate approach in this study of comparing short-period and long-period seismic magnitudes to give a first-order measure of any systematic spectral differences. Teleseismic P wave magnitudes, m_b, compiled by the United States Geological Survey (USGS) National Earthquake Information Center (NEIC) are used as azimuthally averaged measures of relative source strength near 1 s period, and seismic moment magnitudes, M_w, determined from global long-period seismic wave inversions tabulated in the global Centroid-Moment Tensor (gCMT) catalog are used as measures of relative long-period (>30 s) source strength. We compute magnitude differentials, $m_b - M_w$ for events with $M_w \geq 5.0$ for earthquakes with focal mechanisms and locations indicative of megathrust underthrusting events. The gCMT catalog for $M_w \geq 5.0$ is probably quite complete in each of our source areas. Shallow dipping thrust mechanisms with dip values from 10° to 30° were retained. This is performed for the subduction zones where the three great events in Fig. 1 ruptured, as well as for four other subduction zones (Kuril Islands, Aleutian Islands, Southern Sumatra/Sumba, and Peru) where tsunami earthquakes have occurred, indicating some depth-dependent variations. The entire gCMT catalog is considered, using all solutions and USGS magnitudes from January 1976 to August, 2011.

For events with $M_w < 5.0$, relatively few gCMT solutions are available, and the source durations of such events are typically less than 1 s, so m_b and M_w should be equal on average. As seismic moment increases, the source spectrum corner frequency lowers, progressively causing m_b to be lower than M_w yielding $m_b - M_w$ differentials that are increasingly negative. This shift of corner frequency is also accompanied by an intrinsic bias in the routine estimation of m_b for teleseismic short-period P-waves caused by using only the first few seconds of rupture to measure the peak 1-s period amplitude. The source duration exceeds that time window for events larger than about $M_w = 6.5$. For great earthquakes with very long source durations, the m_b and M_w values clearly differ due to these saturation effects (for 2004 Sumatra, $m_b = 6.8$, $m_b - M_w = -2.4$; for 2010 Chile, $m_b = 7.2$, $m_b - M_w = -1.6$; for 2011 Tohoku, $m_b = 7.2$, $m_b - M_w = -1.9$). Thus, using any significant range of earthquake sizes to evaluate spatial patterns in $m_b - M_w$ differences requires a correction of the differential magnitudes for size dependence.

We correct for the saturation effect on $m_b - M_w$ measures using the ω-squared source spectrum scaling of Brune (1970). For this model, the far-field source time function spectrum is given by $D(\omega) = M_o/[1 + (\omega/\omega_c)^2]$, where ω_c is the corner frequency for a given seismic moment, M_o. We can either specify the corner frequency and its seismic moment scaling in terms of a stress parameter, $\omega_c = 2\pi c\beta(\Delta\sigma/M_o)^{0.33}$, where β is shear wave velocity and the constant $c = 0.49$ for SI units, and assume a constant stress parameter $\Delta\sigma$, or we can relate the corner frequency to a characteristic source duration and scale that with M_o. Observationally, we know that a typical $M_w = 6.0$ interplate thrusting event on the central megathrust ($M_o = 1.25 \times 10^{18}$ N m; $M_w = [\log_{10}(M_o) - 9.1]/1.5$) has a duration of about 3 ± 1 s (e.g., Tanioka and Ruff, 1997; Bilek and Lay, 1999), and for self-similar ruptures the duration should approximately scale proportional to $M_o^{0.333}$ (e.g., Aki, 1967; Kanamori and Anderson, 1975). For a reference $M_w = 5.0$; $M_{oref} = 3.94 \times 10^{16}$ N m with duration $t_{ref} = 0.95$ s. Using that reference, the relative 1 s spectral amplitude is computed as a function of M_w using the equations above, and the differential shift relative to M_w is tabulated as a correction to $m_b - M_w$ differentials. Other choices of reference M_w give very similar data trends, and do not affect our conclusions, and use of $M_w = 5.0$ sets a convenient baseline of $m_b - M_w = 0.0$ since the typical corner frequency is expected to be near the period for which m_b is measured. For $M_w = 9.2$ the correction is -1.8, which is generally compatible with the great earthquake observations. This correction is only approximate; for example it assumes that measured M_w is based on true static displacement M_o value when it is typically made in the 30–200 s period band, and that m_b is measured exactly at 1 s period without bias due to using too short of a time window. For $M_w = 6.5$, the $m_b - M_w$ correction is -0.44, and the estimated source duration is just over 5 s, so the procedure used is reasonable for the magnitude range M_w 5.0 to 6.5, and we will constrain our assessment of depth dependence to that range. We find that for that range, the effect of applying the source scaling corrections is very small for any depth-dependent trends because there is substantial scatter and little correlation exists between event size and source depth. We explored using a data base of short-period P wave amplitude measures made using longer time windows for large events (K. Creager, personal communication, 2011), but the number of stations available and the coverage of events in our regions of interest was too limited to extend the magnitude range with unbiased (although still saturated) m_b values.

The event selection process and $m_b - M_w$ differentials, corrected for source spectrum scaling over the full range of M_w (5.0 to 9.0) for the subduction zone near the 2011 Tohoku earthquake are illustrated in Fig. 2. The gCMT best double couple focal mechanisms are plotted at the gCMT centroid locations with colors indicating the centroid depth and symbol sizes scaled proportional to M_w. These events were judged to be interplate megathrust events based on their locations, depths and shallow-dipping thrust mechanisms. The corresponding $m_b - M_w$ measures with corrections are shown on the right map, also plotted at the centroid epicenters and with symbol sizes scaled proportionally to M_w. Redder colors indicate positive $m_b - M_w$ differences, which have relatively more short-period energy than the average source model predicts. These display a tendency to plot closer to the Honshu coastline (down-dip on the megathrust). The bluer colors indicate relatively less short-period energy than the average source model, with the largest, slightly negative value, circle corresponding to the M_w 9.1 2011 Tohoku event. Of course, all of the events differ in finite-source area, and the latter event would tend to reflect some spatial average over the early portion of the expanding rupture for the signal interval in which m_b was measured; it is not a point estimate of the spectral behavior at the centroid location.

Similar plots of gCMT focal mechanisms of selected

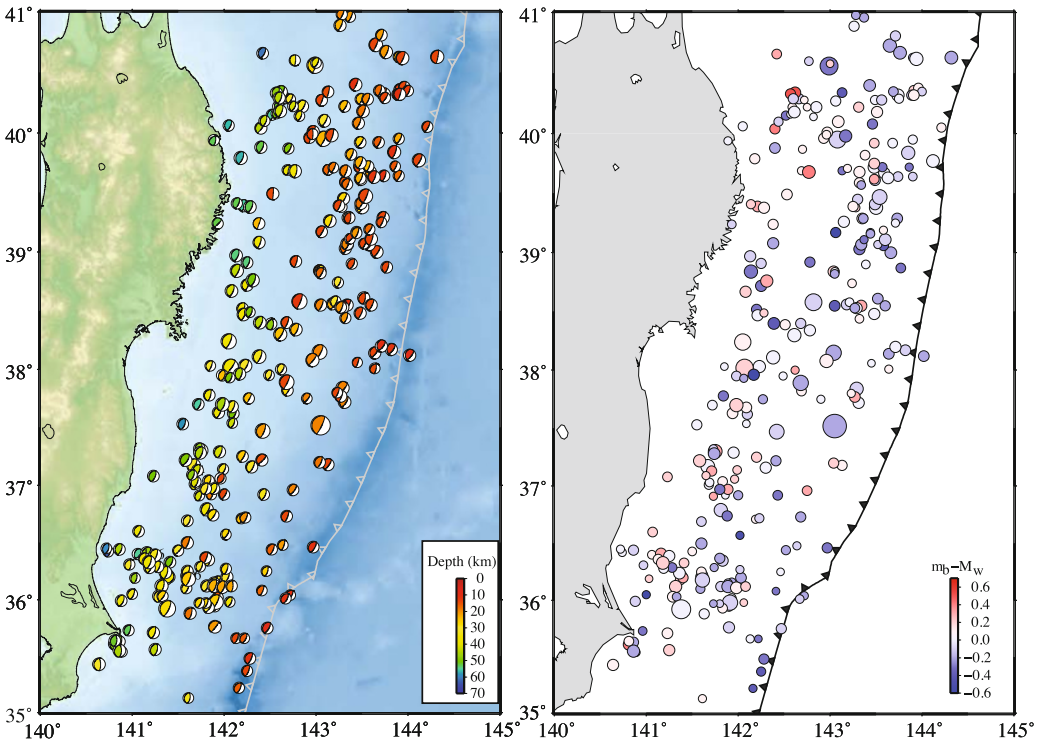

Fig. 2. Maps indicating (left) the locations and global Centroid Moment Tensor (gCMT) focal mechanisms of interplate thrust events probably located on the megathrust along the northeastern Japan subduction zone, colored by centroid depth and with symbol size scaled linearly with seismic moment over the range M_w 5.0 to 9.0, and (right) differences in seismic magnitudes $m_b - M_w$ for these events, with symbol sizes scaled linearly with seismic moment. The magnitude differences have been corrected for corner frequency scaling with seismic moment using an ω-squared source model. The m_b values are from the USGS PDE bulletin and the M_w values are from the gCMT catalog. The data are plotted at the gCMT centroid locations.

events and the corresponding corrected $m_b - M_w$ differences are plotted for the subduction zone regions around the 2004 Sumatra-Andaman earthquake source region (Fig. 3) and the 2010 Chile earthquake source region (Fig. 4). All events are again shown, including the great events for which the centroid locations are not representative of the total depth-range ruptured. There is a clear tendency for the red symbols, indicating positive $m_b - M_w$ (relatively enriched short-period magnitude) to plot down-dip along northern Sumatra, and a corresponding, but weaker, trend along central Chile. There is, however, significant scatter and non-uniformity of coverage. This might allow an interpretation of contribution from along-strike variations as well, but we will focus on the depth trends here given the sparse distributions.

The corrected $m_b - M_w$ differentials for events with M_w in the range 5.0 to 6.5 are plotted as functions of the gCMT centroid depth estimates for the three great earthquake source regions in Fig. 5. The gCMT centroid depths are used because they share any common bias, but the gCMT depth estimates can be 10–20 km deeper than USGS NEIC or JMA hypocentral depths in some regions. The trends of $m_b - M_w$ differentials versus source depth are very similar if we use either of those catalog depth locations instead. The depth-dependent trends apparent in the map views of Figs. 2, 3 and 4 are evident, in that we see positive $m_b - M_w$ differentials at greater depth and overall positive regression slopes, but are obscured by large scatter at each depth. This is not at all unexpected; there is always substantial scatter in seismic magnitude determinations, due to variability in the network average, directivity effects, focal mechanism effects, etc. Nonetheless, the Japan and Sumatra-Andaman data indicate systematic depth variation, and while the Chile data are sparse at larger depths, they are still compatible with a depth dependent increase in relative short-period signal energy. These trends appear to correlate with the depth-dependence in moment-scaled source durations for events larger than 6.0 found by Bilek and Lay (1998, 1999) and Bilek (2007).

One could infer either gradual increases of $m_b - M_w$ with depth or perhaps a step change in constant levels as visible around 37 km deep for the Japan and Sumatra regions. In those two regions, the upper plate has relatively thin crust, so the increase in high frequency content may correspond to transition to mantle/slab contact at around 35 km, which is not the case for Chile, where the upper crust is about 45 km thick. We do not think detailed statistical treatments will provide meaningful assessment given the large scatter and the likely contribution of along-strike heterogeneities, but the basic pattern is compatible with the observations for great ruptures that extend over these full depth ranges; the deeper portion of the megathrust appears to radiate more, or more coherent short-period teleseismic signal for smaller events. It is important to recognize that the back-projection applications intrinsically apply a coherency filter to the short-period data, so they are tuned to detect localized coherent sources and the overall spectral amplitude levels are not determined. Thus, the systematic patterns in the magnitude differences provide new and independent support for depth variations. It is also clear that the sam-

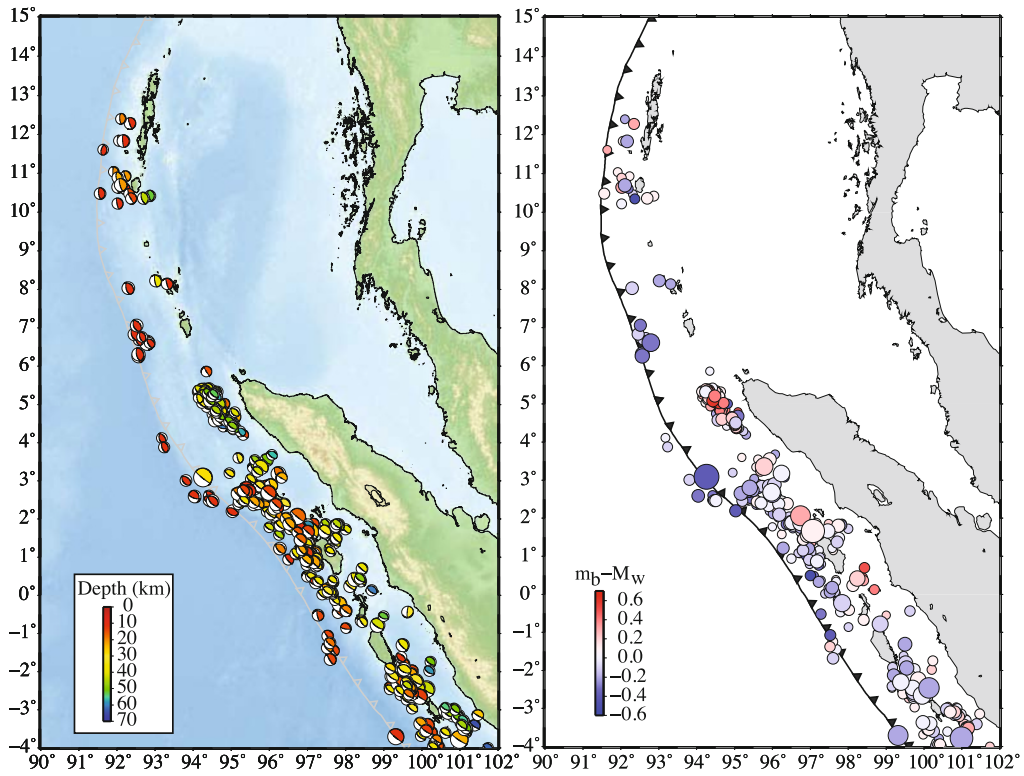

Fig. 3. Maps indicating (left) the locations and global Centroid Moment Tensor (gCMT) focal mechanisms of interplate thrust events probably located on the megathrust along the Sumatra-Andaman subduction zone, colored by centroid depth and with symbol size scaled linearly with seismic moment over the range M_w 5.0 to 9.2, and (right) differences in seismic magnitudes $m_b - M_w$ for these events, with symbol sizes scaled linearly with seismic moment. The magnitude differences have been corrected for corner frequency scaling with seismic moment using an ω-squared source model. The m_b values are from the USGS PDE bulletin and the M_w values are from the gCMT catalog. The data are plotted at the gCMT centroid locations.

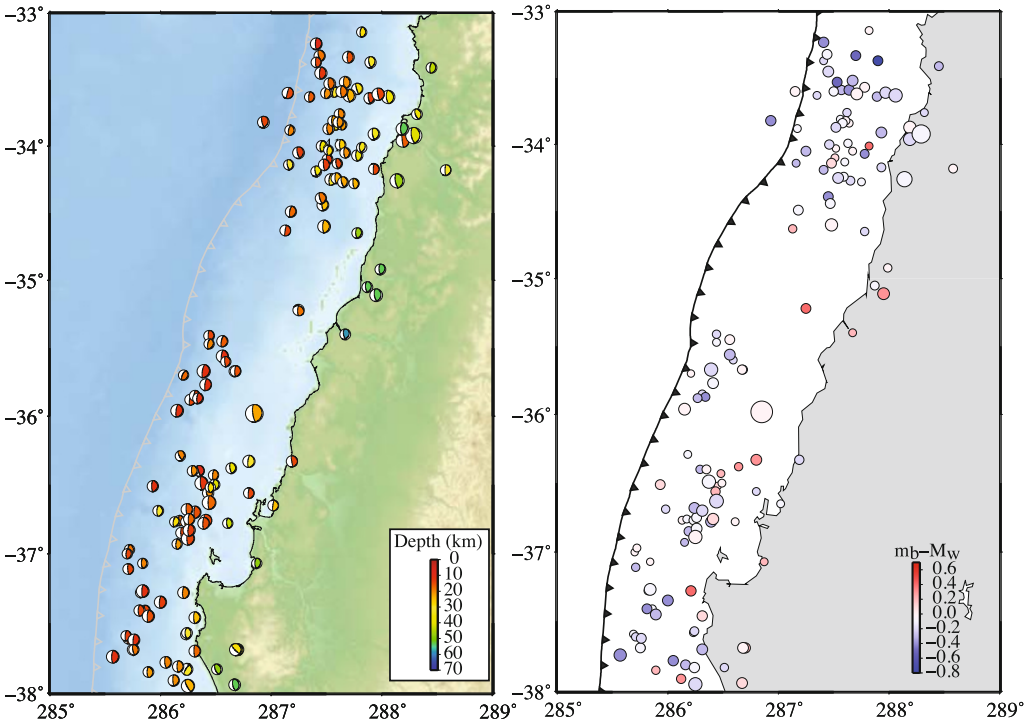

Fig. 4. Maps indicating (left) the locations and global Centroid Moment Tensor (gCMT) focal mechanisms of interplate thrust events probably located on the megathrust along the central Chile subduction zone in the vicinity of the 27 February 2010 Maule earthquake, colored by centroid depth and with symbol size scaled linearly with seismic moment over the range M_w 5.0 to 8.8, and (right) differences in seismic magnitudes $m_b - M_w$ for these events, with symbol sizes scaled linearly with seismic moment. The magnitude differences have been corrected for corner frequency scaling with seismic moment using an ω-squared source model. The m_b values are from the USGS PDE bulletin and the M_w values are from the gCMT catalog. The data are plotted at the gCMT centroid locations.

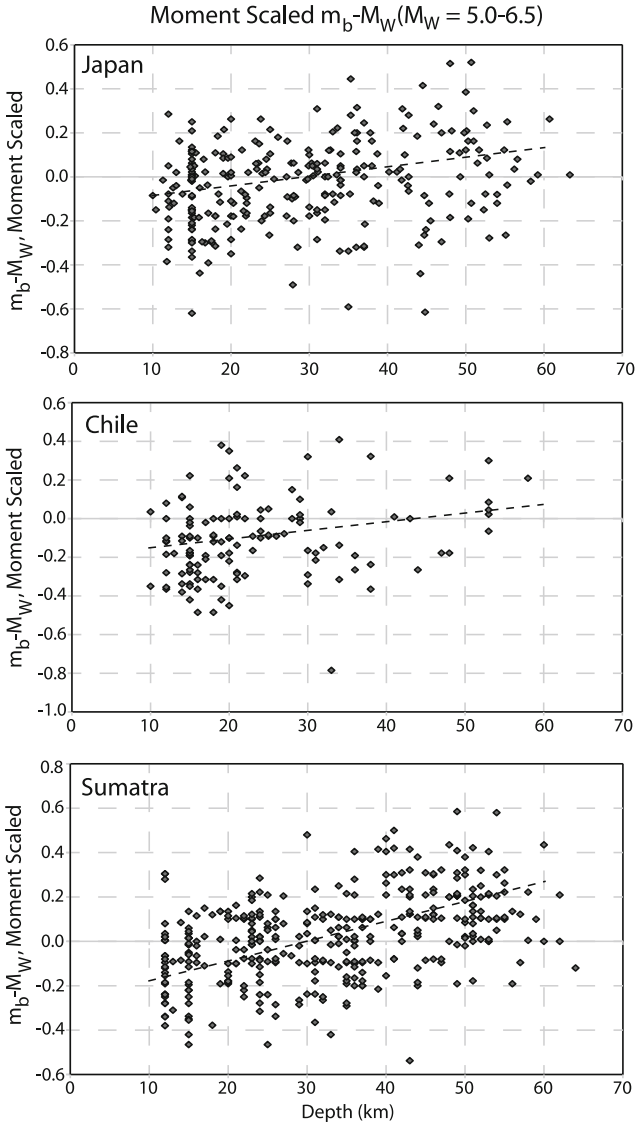

Fig. 5. Depth variation of differences in seismic magnitude differentials $m_b - M_w$ for interplate thrust events on the megathrusts near the 2011 Tohoku, 2004 Sumatra, and 2010 Chile great earthquakes. The magnitude differences have been corrected for corner frequency scaling with seismic moment using an ω-squared source model. The m_b values are from the USGS PDE bulletin and the M_w values are from the gCMT catalog. Only events in the range $5 \leq M_w \leq 6.5$ are included to avoid saturation in the m_b measurements due to fixed time window. Linear regressions over the depth range 10–60 km give the trends indicated by the dashed lines.

pling of the shallowest megathrust region is very limited for events in the selected range of $M_w = 5$ to 6.5; this may be due to the presence of quasi-static slip at shallow depths with rupture of conditionally stable regions only occurring in large tsunami earthquakes that initiate at greater depth and rupture into the shallow portion of the fault. As such, the magnitude differential plots may intrinsically underestimate the total range of variability with depth. We found that the basic patterns were not modified if we included the corrected $m_b - M_w$ values for larger events (M_w 6.5 to 9.2) in these depth comparisons, mainly because they are few in number and are spread over all depths. We omit them here because we are concerned that the large corrections and measurement bias for those events make those data too uncertain.

Similar comparisons of $m_b - M_w$ differentials as functions of gCMT source depth estimates were made for 4 additional regions, all of which have experienced tsunami earthquakes and deeper megathrust events. These are the Kuril Islands-Kamchatka arc from 41° to 55°N, the Aleutian Islands arc from 165° to 210°E, the Peru subduction zone from 0 to 17°S, and the Southern Sumatra/Sunda arc from 100° to 130°E. Interplate thrust events were identified based on the location, depth and gCMT focal mechanisms, and $m_b - M_w$ differences were corrected in the same fashion. The corrected $m_b - M_w$ values for the range of M_w from 5.0 to 6.5 for each region are shown as functions of the gCMT source depth estimates in Fig. 6. Weak trends may be present for the Sumba and the sparsely sampled Peru source regions, but no clear trend is apparent for the well-sampled Kuril and Aleutian arcs and linear regressions did not give significant slope estimates. Maps of data distributions indicate that localized areas along subregions such as Java (also see Bilek and Engdahl, 2007; Convers and Newman, 2011) or Kamchatka may have depth-dependent trends, but the along-arc averaging obscures this as there is large scatter in the data. Since the localized regions tend to have fewer data, we will defer further analysis of other regions to future detailed studies that improve the depth estimates and more fully characterize the source spectra of events on the megathrust. We have not detected any systematic patterns in the depth trends of magnitude residuals with respect to subducting plate age or bathymetric structures, but more detailed analyses should be performed to address that issue rigorously.

4. Discussion and Conclusions

The seismogenic zone is expected to have varying properties as confining pressure and temperature increase, as sediments indurate and undergo phase transitions, as subducted fluids migrate, and as fault roughness from subducted bathymetric topography evolves with increasing depth. The nature of the fault contact also varies from sediment-crust, to crust-crust, to mantle-crust contrasts in lithology. The role that each of these complex factors plays in determining the fault frictional properties that govern seismic wave generation during earthquakes remains obscure. It is perhaps not surprising that earthquake rupture behavior varies with depth, but quantifying what controls the variations is a major challenge.

Use of seismic magnitude measures appears to provide a first-order probe of the depth- and lateral-variations on the megathrust, but the large scatter in magnitude parameters indicates that many other contributions to the observed values need to be accounted for. To the extent that m_b represents the 1 s relative spectral amplitudes, it provides a readily available measure, but short-period radiation is influenced by details of individual ruptures that are not readily quantified, such as directivity, depth phase interference, and source velocity structure. For example, if fault zone rigidity varies systematically with depth along the megathrust, as proposed by Bilek and Lay (1999) and Lay and Bilek (2007), there should be systematic increase in shear velocity with depth, and a concomitant increase in rupture veloc-

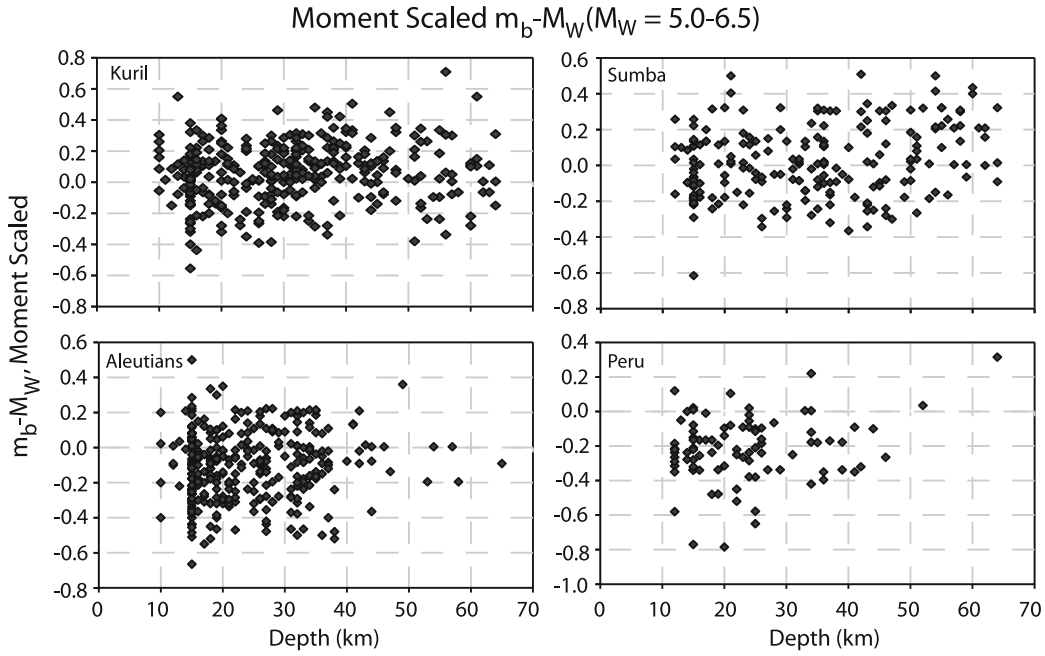

Fig. 6. Depth variation of differences in seismic magnitude differentials $m_b - M_w$ for interplate thrust events on the megathrusts along the Kuril, Sumba, Aleutians and Peru subduction zones. The magnitude differences have been corrected for corner frequency scaling with seismic moment using an ω-squared source model. The m_b values are from the USGS PDE bulletin and the M_w values are from the gCMT catalog. Only events in the range $5 \leq M_w \leq 6.5$ are included to avoid saturation in the m_b measurements due to fixed time window.

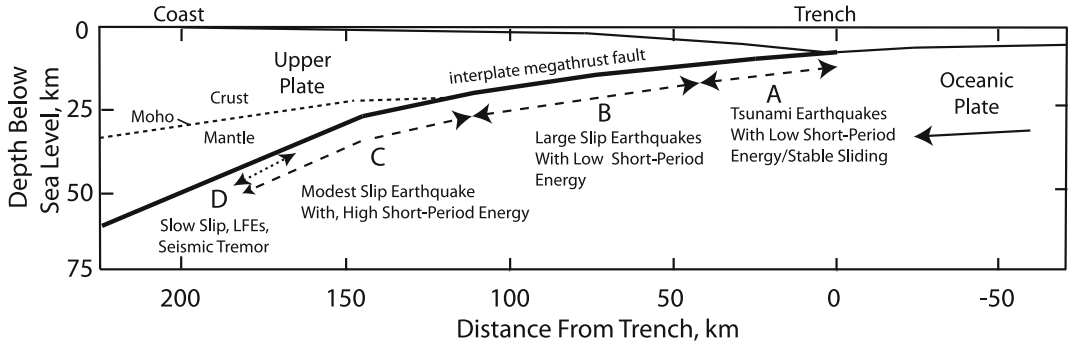

Fig. 7. Rupture domains of interplate megathrust faults. Schematic cross-section, scaled appropriately for the subduction zone off the northeast coast of Honshu where the great 2011 Tohoku earthquake occurred, indicating 4 domains of megathrust rupture characteristics: A—near-trench domain where tsunami earthquakes or anelastic deformation and stable sliding occur; B—central megathrust domain where large slip occurs with minor short-period seismic radiation; C—down-dip domain where moderate slip occurs with significant coherent short-period seismic radiation; D—transitional domain, only present in some areas, typically with a young subducting plate, where slow slip events, low frequency earthquakes (LFEs), and seismic tremor can occur. At yet greater depths the megathrust slides stably or with episodic slow slip or by with plastic deformation that does not generate earthquakes. (From Lay *et al*., 2012).

ity. This could influence the source dimensions for a given moment earthquake, affecting the corner frequency and m_b measures. So, one possible interpretation of the trend of increasing $m_b - M_w$ differential depth in Fig. 5 is that there are smooth or step-wise increases in shear velocity with depth along the megathrust due to progressive sediment induration or lithological contrast changes with depth.

Seismic tomography of the detailed seismogenic fault zone under the overlying wedge (e.g., Kennett *et al*., 2011; Zhao *et al*., 2011) could address this issue independently, but requires fine resolution of the source region that is difficult to obtain. Reflection profiling can also contribute to constraining the velocity structure and layering. For the Japan and Sumatra subduction zones, the depth to the upper plate Moho is about 30 km, so the change from crust-crust to mantle-crust contact might influence the magnitude differences. The Chile zone has a thicker overriding continental crust with Moho depth about 45 km deep, perhaps suppressing the depth-varying behavior relative to the island arcs. The behavior of the other zones that were investigated does not give a clear distinction between island arcs and continental arcs in terms of the depth-dependence of the $m_b - M_w$ differences.

We chose teleseismic measures of the source spectra in order to relate the results to the teleseismic observations for the great earthquake ruptures for which backprojections have been performed. For the Japan source region there are local measures of high frequency magnitude, such as the Japanese Meteorological Agency (JMA) M_J, or Hi-net magnitude, M_{Hinet}, as well as local CMT solutions from

regional wave inversion that provide M_w (regional) estimates. We examined $M_{Hinet} - M_w$ (regional) variations over the Japan subduction zone, motivated by preliminary results by Y. Asano (personal communication, 2011), but the patterns are different from those for $m_b - M_w$ and future work will need to address how m_b and M_{Hinet} or M_J differ in frequency content and event size-scaling behavior. The use of teleseismic magnitude data also allows comparison of regions that do not have dense local seismic networks.

Ultimately, we view the use of magnitude measures as a preliminary step, and feel the best characterization of source variations with position on the megathrust will require full spectral analysis with network isolation of the source spectrum and path/receiver effects, referencing the full spectral behavior to a reference ω-squared model (e.g., Allmann and Shearer, 2009; Bilek *et al*., 2012; Ye *et al*., 2012). However, this study supports the basic inference of some degree of enhanced short-period radiation from down-dip on the megathrust as proposed in the megathrust domain model shown in Fig. 7, from Lay *et al*. (2012). This behavior is detected in both moderate size and great ruptures, so it is an intrinsic feature of the megathrust, not a dynamic rupture attribute. This conceptual framework identifies a shallow Domain A, in which quasi-static slip or tsunami earthquakes occur with very low short-period radiation (and very few moderate size events, so this study does not sample it well), a mid-megathrust Domain B in which large slip can happen in large earthquakes with minor coherent short-period radiation, and a deep-megathrust Domain C which has enriched short-period radiation during failure in isolated events or as part of a great event which ruptures multiple domains. Further along the megathrust there is a transitional Domain D, present in regions with young subducting lithosphere, in which slow slip events, seismic tremor and low frequency earthquakes may occur. There is no direct evidence for Domain D existing in the great earthquake regions examined here, but a transition to stable sliding or anelastic deformation must occur down-dip of Domain C. While simple, this type of conceptual framework does provide a context for further examination of earthquake spectral variations with depth along the megathrust.

Acknowledgments. This work made use of GMT software. The on-line USGS NEIC and Global Centroid-Moment Tensor Catalogs were utilized extensively. We thank guest editor Steve Kirby, Annemarie Baltay and 2 anonymous reviewers for their helpful comments on the manuscript. We thank Ken Creager for directing us to the IRIS measurements of short-period amplitudes for large events. We also thank Y. Asano for providing access to his regional CMT catalog and for examples of his analysis of $M_{Hinet} - M_w$ magnitude differences along Honshu. This work was supported by NSF grant EAR0635570.

References

Aki, K., Scaling law of seismic spectrum, *J. Geophys. Res.*, **72**, 1217–1231, doi:10.1029/JZ072i004p01217, 1967.

Allmann, B. P. and P. M. Shearer, Global variations of stress drop for moderate to large earthquakes, *J. Geophys. Res.*, **114**, B01310, doi:10.1029/2008JB005821, 2009.

Ammon, C. J., C. Ji, H.-K. Thio, D. Robinson, S. Ni, V. Hjorleifsdottir, H. Kanamori, T. Lay, S. Das, D. Helmberger, G. Ichinose, J. Polet, and D. Wald, Rupture process of the great 2004 Sumatra-Andaman earthquake, *Science*, **308**, 1133–1139, 2005.

Ammon, C. J., T. Lay, H. Kanamori, and M. Cleveland, A rupture model of the 2011 off the Pacific coast of Tohoku Earthquake, *Earth Planets Space*, **63**, 693–696, doi:10.5047/eps.2011.05.015, 2011.

Bilek, S. L., Using earthquake source durations along the Sumatra-Andaman subduction system to examine fault-zone variations, *Bull. Seismol. Soc. Am.*, **97**, S62–S70, 2007.

Bilek, S. L. and E. R. Engdahl, Rupture characterization and aftershock relocation for the 1994 and 2006 tsunami earthquakes in the Java subduction zone, *Geophys. Res. Lett.*, **34**, L20311, doi:10.1029/2007GL031357, 2007.

Bilek, S. L. and T. Lay, Variation of interplate fault zone properties with depth in the Japan subduction zone, *Science*, **281**, 1175–1178, 1998.

Bilek, S. L. and T. Lay, Rigidity variations with depth along interplate megathrust faults in subduction zones, *Nature*, **400**, 443–446, 1999.

Bilek, S. L. and T. Lay, Tsunami earthquakes: Possibly widespread manifestations of frictional conditional stability, *Geophys. Res. Lett.*, **29**(14), doi:10.1029/2002GL015215, 2002.

Bilek, S. L., H. R. DeShon, and E. R. Engdahl, Spatial variations in earthquake source characteristics within the 2011 Mw = 9.0 Tohoku, Japan rupture zone, *Geophys. Res. Lett.*, **39**, L09304, doi:10.1029/2012GL051399, 2012.

Brune, J. N., Tectonic stress and the spectra of seismic shear waves from earthquakes, *J. Geophys. Res.*, **75**, 4997–5009, 1970.

Chlieh, M., J.-P. Avouac, V. Hjorleifsdottir, T.-R. A. Song, C. Ji, K. Sieh, A. Sladen, H. Hebert, L. Prawirodirdjo, Y. Bock, and J. Galetzka, Coseismic slip and afterslip of the great M_w 9.15 Sumatra-Andaman Earthquake of 2004, *Bull. Seismol. Soc. Am.*, **97**, S152–S173, 2007.

Convers, J. A. and A. V. Newman, Global evaluation of large earthquake energy from 1997 through mid-2010, *J. Geophys. Res.*, **116**, B08304, doi:10.1029/2010JB007928, 2011.

Fujii, Y., K. Satake, S. Sakai, M. Shinohara, and T. Kanazawa, Tsunami source of the 2011 off the Pacific coast of Tohoku Earthquake, *Earth Planets Space*, **63**, 815–820, doi:10.5047/eps.2011.06.010, 2011.

Hayes, G. P., Rapid source characterization of the 2011 M_w 9.0 off the Pacific coast of Tohoku Earthquake, *Earth Planets Space*, **63**, 529–534, doi:10.5047/eps.2011.05.012, 2011.

Ide, S., A. Baltay, and G. C. Beroza, Shallow dynamic overshoot and energetic deep rupture in the 2011 M_w 9.0 Tohoku-oki earthquake, *Science*, **332**, 1426–1429, 2011.

Iinuma, T., M. Ohzono, Y. Ohta, and S. Miura, Coseismic slip distribution of the 2011 off the Pacific coast of Tohoku Earthquake (M 9.0) estimated based on GPS data—Was the asperity in Miyagi-oki ruptured?, *Earth Planets Space*, **63**, 643–648, doi:10.5047/eps.2011.06.013, 2011.

Ishii, M., High-frequency rupture properties of the M_w 9.0 off the Pacific coast of Tohoku Earthquake, *Earth Planets Space*, **63**, 609–614, doi:10.5047/eps.2011.07.009, 2011.

Ishii, M., P. M. Shearer, H. Houston, and J. E. Vidale, Extent, duration and speed of the 2004 Sumatra-Andaman earthquake imaged by the Hi-net array, *Nature*, **435**, 933–936, 2005.

Ito, T., K. Ozawa, T. Watanabe, and T. Sagiya, Slip distribution of the 2011 off the Pacific coast of Tohoku Earthquake inferred from geodetic data, *Earth Planets Space*, **63**, 627–630, doi:10.5047/eps.2011.06.023, 2011.

Kanamori, H., Mechanism of tsunami earthquakes, *Phys. Earth Planet. Inter.*, **6**, 246–259, 1972.

Kanamori, H., Rupture process of subduction-zone earthquakes, *Ann. Rev. Earth Planet. Sci.*, **14**, 293–322, 1986.

Kanamori, H. and D. L. Anderson, Theoretical basis of some empirical relations in seismology, *Bull. Seismol. Soc. Am.*, **65**, 1073–1095, 1975.

Kanamori, K. and M. Kikuchi, The 1992 Nicaragua earthquake: A slow tsunami earthquake associated with subducted sediments, *Nature*, **361**, 714–716, 1993.

Kennett, B. L. N., A. Gorbatov, and E. Kiser, Structural controls on the M_w 9.0 2011 Offshore-Tohoku earthquake, *Earth Planet. Sci. Lett.*, **310**, 462–467, 2011.

Kikuchi, M. and Y. Fukao, Inversion of long-period P-waves from great earthquakes along subduction zones, *Tectonophysics*, **144**, 231–247, 1987.

Kiser, E. and M. Ishii, The 2010 M_w 8.8 Chile earthquake: Triggering on multiple segments and frequency-dependent rupture behavior, *Geophys. Res. Lett.*, **38**, L07301, doi:10.1029/2011GL047140, 2011.

Koketsu, K., Y. Yokota, N. Nishimura, Y. Yagi, S. Miyazaki, K. Satake, Y. Fujii, H. Miyake, S. Sakai, Y. Yamanaka, and T. Okada, A unified source model for the 2011 Tohoku earthquake, *Earth Planet. Sci. Lett.*, **310**, 480–487, 2011.

Koper, K. D., A. R. Hutko, and T. Lay, Along-dip variation of teleseismic short-period radiation from the 11 March 2011 Tohoku Earthquake (M_w

9.0), *Geophys. Res. Lett.*, **38**, L21309, doi:10.1029/2011GL049689, 2011a.

Koper, K. D., A. R. Hutko, T. Lay, C. J. Ammon, and H. Kanamori, Frequency-dependent rupture process of the 2011 M_w 9.0 Tohoku Earthquake: Comparison of short-period P wave backprojection images and broadband seismic rupture models, *Earth Planets Space*, **63**, 599–602, doi:10.5047/eps.2011.05.026, 2011b.

Koper, K. D., A. R. Hutko, T. Lay, and O. Sufri, Imaging short-period seismic radiation from the 27 February 2010 Chile (M_w 8.8) earthquake by back-projection of P, PP, and PKIKP waves, *J. Geophys. Res.*, **117**, B02308, doi:10.1029/2011JB008576, 2012.

Krüger, F. and M. Ohrnberger, Tracking the rupture of the $M_w = 9.3$ Sumatra earthquake over 1150 km at teleseismic distance, *Nature*, **435**, 937–939, 2005.

Kurahashi, S. and K. Irikura, Source model for generating strong ground motions during the 2011 off the Pacific coast of Tohoku Earthquake, *Earth Planets Space*, **63**, 571–576, doi:10.5047/eps.2011.06.044, 2011.

Lay, T. and S. Bilek, Anomalous earthquake ruptures at shallow depths on subduction zone megathrusts, in *The Seismogenic Zone of Subduction Thrust Faults*, edited by T. H. Dixon and J. C. Moore, pp. 476–511, Columbia University Press, New York, 2007.

Lay, T., H. Kanamori, and L. J. Ruff, The asperity model and the nature of large subduction zone earthquakes, *Earthq. Predict. Res.*, **1**, 3–71, 1982.

Lay, T., C. J. Ammon, H. Kanamori, K. D. Koper, O. Sufri, and A. R. Hutko, Teleseismic inversion for rupture process of the 27 February 2010 Chile (M_w 8.8) earthquake, *Geophys. Res. Lett.*, **37**, L13301, doi:10.1029/2010GL043379, 2010.

Lay, T., C. J. Ammon, H. Kanamori, L. Xue, and M. J. Kim, Possible large near-trench slip during the 2011 M_w 9.0 off the Pacific coast of Tohoku Earthquake, *Earth Planets Space*, **63**, 687–692, doi:10.5047/eps.2011.05.033, 2011.

Lay, T., H. Kanamori, C. J. Ammon, K. D. Koper, A. R. Hutko, L. Ye, H. Yue, and T. M. Rushing, Depth-varying rupture properties of subduction zone megathrust faults, *J. Geophys. Res.*, **117**, B04311, doi:10.1029/2011JB009133, 2012.

Lee, S.-J., B.-S. Huang, M. Ando, H.-C. Chiu, and J.-H. Wang, Evidence of large scale repeating slip during the 2011 Tohoku-oki earthquake, *Geophys. Res. Lett.*, **38**, L19306, doi:10.1029/2011GL049580, 2011.

Lorito, S., F. Romano, S. Atzori, X. Tong, A. Avallone, J. McCloskey, E. Boschi, and A. Piatanesi, Limited overlap between the seismic gap and coseismic slip of the great 2010 Chile earthquake, *Nat. Geosci.*, **4**, 173–177, 2011.

Maeda, T., T. Furumura, S. Sakai, and M. Shinohara, Significant tsunami observed at ocean-bottom pressure gauges during the 2011 off the Pacific coast of Tohoku Earthquake, *Earth Planets Space*, **63**, 803–808, doi:10.5047/eps.2011.06.005, 2011.

Meng, L., A. Inbal, and J.-P. Ampuero, A window into the complexity of the dynamic rupture of the 2011 M_w 9 Tohoku-oki earthquake, *Geophys. Res. Lett.*, **38**, L00G07, doi:10.1029/2011GL048118, 2011.

Newman, A. V. and E. A. Okal, Teleseismic estimates of radiated seismic energy: The E/M_o discriminant for tsunami earthquakes, *J. Geophys. Res.*, **103**, 26,885–26,898, 1998.

Ozawa, S., T. Nishimura, H. Suito, T. Kobayahi, M. Tobita, and T. Imakiire, Coseismic and postseismic slip of the 2011 magnitude-9 Tohoku-Oki earthquake, *Nature*, **475**, 373–376, doi:10.1038/nature10227, 2011.

Ozawa, S., T. Nishimura, H. Munekane, H. Suito, T. Kobayashi, M. Tobita, and T. Imakiire, Preceding, coseismic, and postseismic slips of the 2011 Tohoku earthquake, Japan, *J. Geophys. Res.*, **117**, B07404, doi:10.1029/2011JB009120, 2012.

Poisson, B., C. Oliveros, and R. Pedreros, Is there a best source model of the Sumatra 2004 earthquake for simulating the consecutive tsunami?, *Geophys. J. Int.*, doi:10.1111/j.1365-246X.2011.05009.x, 2011.

Polet, J. and H. Kanamori, Shallow subduction zone earthquakes and their tsunamigenic potential, *Geophys. J. Int.*, **142**, 684–702, 2000.

Pollitz, F., R. Bürgmann, and P. Banerjee, Geodetic slip model of the 2011 M 9.0 Tohoku earthquake, *Geophys. Res. Lett.*, **38**, L00G08, doi:10.1029/2011GL048632, 2011a.

Pollitz, F. F., B. Brooks, X. Tong, M. G. Bevis, J. H. Foster, R. Bürgmann *et al.*, Coseismic slip distribution of the February 27, 2010 M_w 8.8 Maule, Chile earthquake, *Geophys. Res. Lett.*, **38**, L09309, doi:10.1029/2011GL047065, 2011b.

Rhie, J., D. Dreger, R. Burgmann, and B. Romanowicz, Slip of the 2004 Sumatra-Andaman earthquake from joint inversion of long-period global seismic waveforms and GPS static offsets, *Bull. Seismol. Soc. Am.*, **97**(1A), S115–S127, 2007.

Shao, G., X. Li, C. Ji, and T. Maeda, Focal mechanism and slip history of the 2011 M_w 9.1 off the Pacific coast of Tohoku Earthquake, constrained with teleseismic body and surface waves, *Earth Planets Space*, **63**, 599–564, doi:10.5047/eps.2011.06.028, 2011.

Simons, M., S. E. Minson, A. Sladen, F. Ortega, J. Jiang, S. E. Owen, *et al.*, The 2011 magnitude 9.0 Tohoku-oki earthquake: Mosaicking the megathrust from seconds to centuries, *Science*, **332**, 1421–1425, 2011.

Tanioka, Y. and L. J. Ruff, Source time functions, *Seismol. Res. Lett.*, **68**, 386–400, 1997.

Vigny, C., W. J. F. Simons, S. Abu, R. Bamphenyu, C. Satirapod, N. Choosakul, C. Subarya, A. Socquet, K. Omar, H. Z. Abidin, and B. A. C. Ambrosius, Insight into the 2004 Sumatra-Andaman earthquake from GPS measurements in southeast Asia, *Nature*, **436**, 201–206, 2005.

Vigny, C., A. Socquet, S. Peyrat, J.-C. Ruegg, M. Metois, R. Madariaga *et al.*, The 2010 M_w 8.8 Maule mega-thrust earthquake of central Chile, monitored by GPS, *Science*, **332**, 1417–1421, 2011.

Wang, D. and J. Mori, Rupture process of the 2011 off the Pacific coast of Tohoku Earthquake (M_w 9.0) as imaged with back-projection of teleseismic P-waves, *Earth Planets Space*, **63**, 603–607, doi:10.5047/eps.2011.05.029, 2011a.

Wang, D. and J. Mori, Frequency-dependent energy radiation and fault coupling for the 2010 M_w 8.8 Maule, Chile and 2011 M_w 9.0 Tohoku, Japan earthquakes, *Geophys. Res. Lett.*, **38**, L22308, doi:10.1029/2011GL049652, 2011b.

Wei, S., R. Graves, D. Helmberger, J.-P. Avouac, and J. Jiang, Sources of shaking and flooding during the Tohoku-Oki earthquake: A mixture of rupture styles, *Earth Planet. Sci. Lett.*, **333–334**, 91–100, 2012.

Yamanaka, Y. and M. Kikuchi, Asperity map along the subduction zone in northeastern Japan inferred from regional seismic data, *J. Geophys. Res.*, **109**, B07307, 2004.

Yao, H., P. Gerstoft, P. M. Shearer, and C. Mecklenbrauker, Compressive sensing of the Tohuku-Oki M_w 9.0 earthquake: Frequency-dependent rupture modes, *Geophys. Res. Lett.*, **38**, doi:10.1029/2011GL049223, 2011.

Ye, L., T. Lay, and H. Kanamori, Ground shaking and seismic source spectra for large earthquakes around the megathrust fault offshore of northeastern Honshu, Japan, *Bull. Seismol. Soc. Am.*, 2012 (in press).

Yokota, Y., K. Koketsu, Y. Fujii, K. Satake, S. Sakai, M. Shinohara, and T. Kanazawa, Joint inversion of strong motion, teleseismic, geodetic, and tsunami datasets for the rupture process of the 2011 Tohoku earthquake, *Geophys. Res. Lett.*, **38**, L00G21, doi:10.1029/2011GL050098, 2011.

Yomogida, K., K. Yoshizawa, J. Koyama, and M. Tsuzuki, Along-dip segmentation of the 2011 off the Pacific coast of Tohoku Earthquake and comparison with other megathrust earthquakes, *Earth Planets Space*, **63**, 697–701, doi:10.5047/eps.2011.06.003, 2011.

Yoshida, Y., H. Ueno, D. Muto, and S. Aoki, Source process of the 2011 off the Pacific coast of Tohoku Earthquake with the combination of teleseismic and strong motion data, *Earth Planets Space*, **63**, 565–569, doi:10.5047/eps.2011.05.011, 2011.

Yue, H. and T. Lay, Inversion of high-rate (1-sps) GPS data for rupture process of the 11 March 2011 Tohoku earthquake (Mw 9.1), *Geophys. Res. Lett.*, **38**, L00G09, doi:10.1029/2011GL048700, 2011.

Zhang, H., Z. Ge, and L. Ding, Three sub-events composing the 2011 off the Pacific coast of Tohoku Earthquake (M_w 9.0) inferred from rupture imaging by back-projecting teleseismic P waves, *Earth Planets Space*, **63**, 595–598, doi:10.5047/eps.2011.06.021, 2011.

Zhao, D., Z. Huang, N. Umino, A. Hasegawa, and H. Kanamori, Structural heterogeneity in the megathrust zone and mechanism of the 2011 Tohoku-oki earthquake (M_w 9.0), *Geophys. Res. Lett.*, **38**, L17308, doi:10.1029/2011GL048408, 2011.

T. M. Rushing and T. Lay (e-mail: tlay@ucsc.edu)